

TEST OF FOCUS

Spartan Infrared Camera for the SOAR Telescope

Dustin Baker, Brandon Hanold, Edwin D. Loh
Department of Physics & Astronomy
Michigan State University, East Lansing, MI 48824

Loh@msu.edu

517 355-9200 ext 2480

26 August 2005

We measured the focus of the instrument by imaging a pinhole on the mask. To focus, the pinhole must be moved 3.03 ± 0.06 mm for the f/12 channel and 0.79 ± 0.05 mm for the f/21 channel. We discovered many problems in positioning the optics. These problems account for most of the shift: the residual is 0.02 mm for the f/12 channel and -0.19 mm for the f/21 channel. Because the residuals are small and the Strehl ratio is high, we are confident that the optics will be positioned correctly when the problems are fixed.

1 Introduction

To determine the image quality of the instrument, we imaged a pinhole illuminated by a 632-nm laser. We found that the Strehl ratio is only 2% lower than the design goal for f/12 and 11% for f/21 at 632nm.¹ However, to focus, the pinhole had to be moved by 3.0 mm for f/12 and 0.8 mm for f/21. Here we aim to discover why the focus shifted so much.



Figure 1 Images¹ in the f/21 channel (top) and the f/12 channel (bottom) of an 8- μ m pinhole illuminated with a 632-nm laser. The geometrical image of the pinhole is the smaller circle. The first dark diffraction ring for 632 nm is the larger circle, which is twice as large for the J band.

¹ Baker, D., Hanold, B., & Loh, E., December 2004, "Measurement of the Image Quality, Spartan IR Camera for the SOAR Telescope," unpublished.

1.1 Coordinates

Two local coordinate systems are used. (Local means the coordinate system is tied to the optic.) The primary system is defined by the normal vector \mathbf{n} of the optic and the \mathbf{z} vector, which points from the bottom of the cryo-optical box (COB) to the top. The \mathbf{z} vector points out of the paper in Figure 2. The third vector is $\mathbf{n} \times \mathbf{z}$. Zemax,

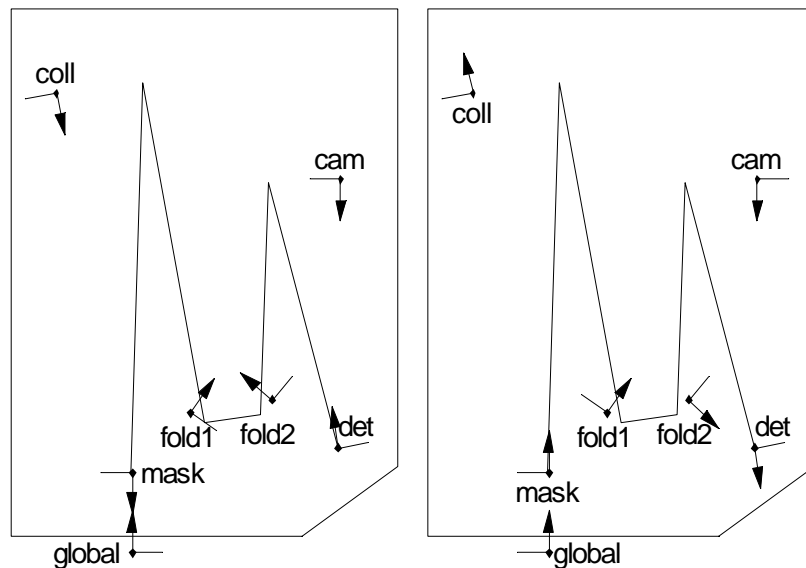


Figure 2 Left: Primary local coordinates. The arrow is the normal \mathbf{n} of the optic; the line is $\mathbf{n} \times \mathbf{z}$, where \mathbf{z} is the unit vector pointing out of the paper. For the global coordinate system, the line is the x-axis, and the arrow is the y-axis. Right: Local coordinates used by Zemax. The arrow is the z_z -axis; line is the y_z -axis. The long, continuous line is a ray. The f/12 channel is shown.

the optical design program, uses a local coordinate system $\mathbf{x}_z, \mathbf{y}_z, \mathbf{z}_z$ for which the z_z -direction reverses at each reflection. The \mathbf{x}_z vector points into the paper in Figure 2.

The global coordinate systems are also shown in Figure 2.

1.2 Locating Features

Pads and pins—two in the bottom of the COB, one in the top, and two on the optic—fix the position of the optic. Shims between the optical assembly and the COB allow movement to compensate for fabrication errors. See Figure 3 for the f/12 collimator and the f/12 camera assembly. The other optics are similar. The fold mirrors do not have pins, since they are flat.

2 Measurement of Optics in the Cryo-optical Box

We measured the positions of the optics installed in the bottom of cryo-optical box. We measured the surface of the mask wheel, the pads and pins of the f/12 collimator, the backs of the posts for the fold mirrors, the pads and pins of the f/12 camera mirror, and the pads and pins of the f/21 camera mirror. The f/21 collimator assembly was not available, because the rotation stage was being repaired. Since the rotation stage for the f/12 camera was removed for testing and reinstalled without realigning, the position of the f/12 camera is not true.

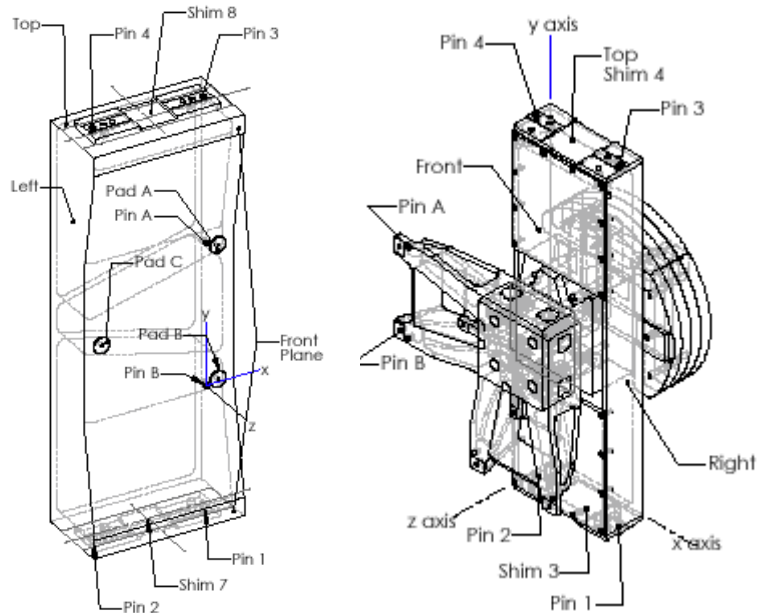


Figure 3 Features that fix the position of the f/12 collimator (left) and f/12 camera (right). Left: Pins 1, 2, and 3 mate the f/12 collimator post to the COB. Pins A and B and pads A, B, and C mate the optic to the post. Shims 7 and 8 are positioned during alignment and bolted on the post. Right: Pins 1, 2, and 3 mate the f/12 camera assembly to the COB. Pins A and B and three pads mate the optic to the post. Shims 3 and 4 are positioned during alignment and bolted on the post.

2.1 Pins in the COB

Since the top of the COB was removed to access the optics, we measured the pins in the top and the mating pins in the optical assemblies in order to infer the true positions. We discovered that the top plate of the COB is rotated by 0.107 mrad and translated by (0.005, 0.003) mm with respect to its position as measured in 2003. (See Figure 4.) There is also a scale change of 1.00002, which could be caused by a temperature change of +1C. The measurement of the right pin for the f/12 camera is 0.026 mm from its location in 2003; the recent measurement is probably incorrect, since the spacing between the left and right pins has changed significantly from the nominal value. Without that point, the standard deviation of the residual $(\sigma_x, \sigma_y) = (0.003, 0.004)$ mm. The rotation is significant; the shift is insignificant.

We will not correct the rotation of the top plate of the COB, since the rotation is 57% of the tightest tolerance, which is that for fold mirror #1. Furthermore it is possible that a rotation of the entire top plate, rather than a single mirror, allows a looser tolerance.

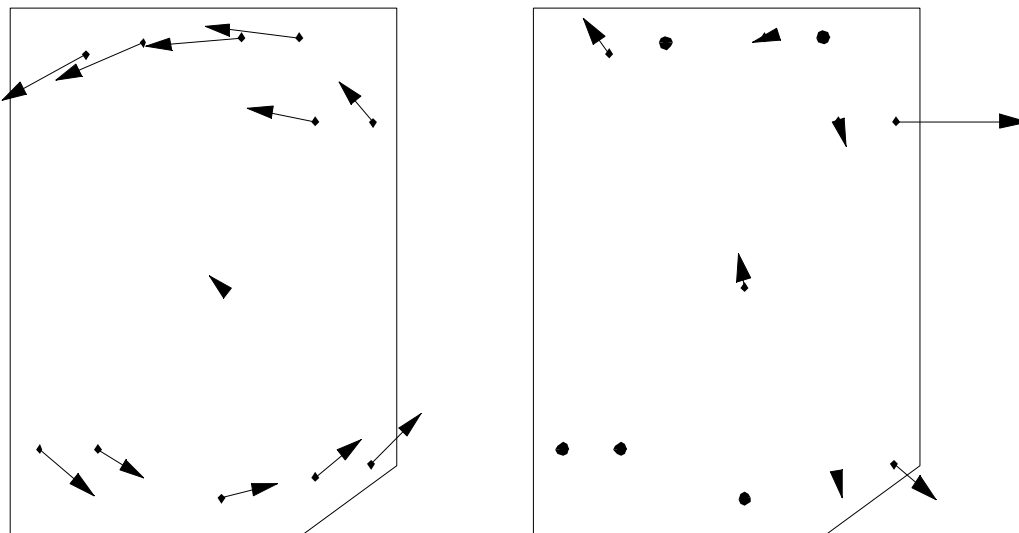


Figure 4 Left: Shift (magnified by $\times 3k$) in the pins on the top of the COB with respect to their positions in 2003. The largest shift is 0.06 mm. Right: Shift (magnified by 10k) after rotating counter clockwise by 0.107 mrad and scaling by 1.000021 about the point (150,400) and translating by (0.005, 0.003). the largest shift is 0.025 mm.

2.2 Pins in optics

Two pins in each optical assembly define the location of the optic in the direction perpendicular to the axis, and the positional errors of the pins are in Table 1. Since the rotation stage for f/12 camera was removed for testing and installed without realigning, its position is not accurate.

Table 1 Positioning of the optics in the COB in the direction perpendicular to the axis of the optic.

| Pin | Meas. position | | | | Design change | Residual err | | | Resid/Tol | |
|-----------------|----------------|--------|-------|-------|---------------|--------------|-------|-------|-----------|------|
| | u | z | err u | err z | | du | u | z | u | z |
| f12Col-T | -176.60 | 72.00 | -0.60 | 0.00 | Shift pins | -0.46 | -0.14 | 0.00 | -0.1 | 0.0 |
| f12Col-B | -176.55 | -72.00 | -0.55 | 0.00 | | | -0.09 | 0.00 | -0.1 | 0.0 |
| f12Cam-T | 140.88 | 51.27 | 2.38 | -0.73 | Shift pins | 1.50 | 0.47 | 0.41 | 0.2 | 1.7 |
| f12Cam-B | 140.04 | -52.67 | 1.54 | -0.67 | | | 0.46 | 0.46 | 0.2 | 1.9 |
| f21Cam-T | 133.79 | 52.00 | 0.47 | 0.00 | Shift pins | 0.46 | 0.01 | 0.00 | 0.1 | 0.0 |
| <u>f21cam-B</u> | <u>133.80</u> | -52.05 | 0.48 | -0.05 | | | 0.03 | -0.05 | 0.1 | -0.3 |

z that of global coordinate system

u $n \times z$

The locations of the pins reveal errors in the positioning of the f/12 collimator, f/12 camera, and f/21 camera. The pins in the COB were fabricated with an outdated mechanical design. We fixed this by moving the shims to compensate. With this change, the lateral positions of the f/12 collimator and f/21 camera mirror meet the requirements (See the last two columns of Table 1).

2.3 Tilt of the Optics

Pads define the direction of the axis of an optic, which is the symmetry axis for a surface of rotation. Since the pads of the fold mirrors are inaccessible, we measured the backs of the fold posts instead. For the mask, we measured the mask wheel. The error (Table 2) is defined to be $\mathbf{t} \times \mathbf{m}$, the cross product of the target \mathbf{t} and measured axis \mathbf{m} . The direction of $\mathbf{t} \times \mathbf{m}$ is the rotation axis, and the magnitude is the angle.

Table 2 Axes of the optical elements measured in the cryo-optical box. The rotation $\mathbf{t} \times \mathbf{m}$, the cross product of the target \mathbf{t} and measured axis \mathbf{m} , expressed in column 3 as a rotation about the z axis, which is perpendicular to the top of the COB, and in column 4 as a rotation about the $\mathbf{t} \times \mathbf{z}$ axis. The rotation caused by errors in the alignment are in columns 4 and 5. The rotation of the whole top of the COB is in column 6. The residual rotation is in columns 7 and 8. The ratio of the residual error to the tolerance is in the last two columns.

| | $\mathbf{t} \times \mathbf{m}$ | | $\mathbf{t} \times \mathbf{m}$ inAlign | | $\mathbf{t} \times \mathbf{m}$ inCOB | $\mathbf{t} \times \mathbf{m}$ residual | | | |
|------------------|--------------------------------|-------|----------------------------------------|-------|--------------------------------------|-----------------------------------------|-------|-------|-------|
| | u | z | u | z | u | u | z | u/tol | z/tol |
| | mrاد | mrاد | mrاد | mrاد | mrاد | mrاد | mrاد | | |
| (1) | (2) | (3) | (4) | (5) | (6) | (7) | (8) | (9) | (10) |
| f12Col | -0.64 | 0.75 | -0.25 | 0.92 | 0.12 | -0.52 | -0.18 | -2.1 | -0.4 |
| f12Cam | 1.23 | -1.43 | 0.02 | -0.09 | -0.08 | 1.3 | -1.3 | 5.6 | -4.5 |
| mask | -0.15 | 1.18 | -0.38 | -0.05 | 0.04 | 0.2 | 1.2 | 0.0 | 0.2 |
| f21Cam | 0.03 | -0.37 | -0.03 | -0.29 | 0.04 | 0.02 | -0.08 | 0.1 | -0.2 |
| backFold1 | -0.12 | 0.85 | -0.13 | 0.67 | | 0.01 | 0.18 | 0.0 | 1.0 |
| <u>backFold2</u> | 0.07 | 0.96 | 0.27 | 0.61 | | -0.21 | 0.35 | -0.9 | 0.9 |
| \mathbf{t} | target | | | | | | | | |
| \mathbf{m} | measured | | | | | | | | |
| u | $\mathbf{t} \times \mathbf{z}$ | | | | | | | | |

The top plate of the COB has a small rotation.

2.3.1 f/12 Collimator

The f/21 collimator post was clamped improperly during alignment so as to introduce a twist.

In the z direction the residual rotation is within tolerance, but it is not in the transverse ($\mathbf{n} \times \mathbf{z}$) direction. (See last two columns in Table 2.) It is possible that bumping the post during measurement in the COB moved it. Bolted only at the bottom, the post is not immune to tilt in the transverse direction.

2.3.2 f/12 Camera Mirror

Improper compensation for fabrication errors in the COB tilts the f/12 camera mirror slightly.

Since the rotation stage used to support the mirror arm was loose at this time (before it was remanufactured), the large tilt is not unexpected.

2.3.3 Mask Wheel

Improper compensation for fabrication errors in the COB tilts the mask wheel slightly.

The large tilt is probably due to the loose rotation stage.

2.3.4 f/21 Camera Mirror

Two errors account completely for the tilt of the f/21 camera mirror. Improper compensation for fabrication errors in the COB tilts the f/21 camera mirror slightly. The f/21 collimator post was clamped improperly during alignment so as to introduce a twist.

2.3.5 Fold 1

Improper compensation for fabrication errors during alignment accounts completely for the tilt.

2.3.6 Fold 2

Even after accounting for improper compensation for fabrication errors during alignment, large residuals remain for Fold 2. An alignment error, noted but not corrected, may account for the residuals.

2.4 Positioning Parallel to the Axis of the Optic

The positional errors in the direction of the element axis are in Table 1.

2.4.1 f/12 Collimator

The f/21 collimator post was clamped improperly during alignment so as to introduce a shift.

Table 3 Position of optics in direction of the element axis. The parameter n is the signed distance from the vertex of the optic to the plane of the measured pads (the back in the case of the fold mirrors). A positive n is in the direction of the out-facing normal.

| | n | dn | Correction | | |
|---------------------|---------|--------|----------------------------|--------|--------|
| | | | | dn | Resid |
| f12Col | 38.639 | 0.016 | Clamping | 0.017 | -0.001 |
| f12Cam | 29.104 | -0.119 | Alignment spec. & Tilt | 0.106 | -0.225 |
| mask | 0.550 | 0.550 | Alignment spec. & Tilt | 0.540 | 0.010 |
| f21Cam | 29.268 | 0.045 | Clamping & Alignment spec. | -0.051 | 0.096 |
| backFold1 wrt fold1 | -33.781 | 0.696 | Alignment spec. | 0.624 | 0.072 |
| backFold2 wrt fold2 | -33.963 | 0.514 | Alignment spec. | 0.565 | -0.051 |

2.4.2 f/12 Camera Mirror

Improper compensation for fabrication errors in the COB shifts the f/12 camera mirror. Furthermore the arm moves between the orientation used for alignment and the orientation used in the COB, because the direction of gravity is different and the rotation stage was loose.

The large residual may be due to hysteresis of the rotation stage. With a second measurement of the tilt, the residual changes from -0.23 to -0.14 mm.

2.4.3 Mask Wheel

The alignment instructions did not account for the error in the thickness of the mask wheel. Improper compensation for fabrication errors in the COB moves the mask wheel slightly. Lastly, the wheel tilted, because the rotation stage was loose.

2.4.4 f/21 Camera Mirror

Two errors account completely for the tilt of the f/21 camera mirror. Improper compensation for fabrication errors in the COB shifts the f/21 camera mirror slightly. The f/21 collimator post was clamped improperly during alignment so as to introduce a shift.

2.4.5 Fold 1 and 2

In the mechanical design, the mirror blank, rather than the finished mirror was used. In addition, the mirror post was clamped improperly when it was measured.

3 Measurement of the Mirrors with a CMM

We measured the mirrors (except for the flat ones) on a coordinate measuring machine (CMM) at Coordinate Measurement Specialists in Wixom, MI. The CMM is a Zeiss UMC850, which is calibrated to $0.5\mu\text{m}$ over the volume. The mirrors were mounted on the jig that was used for fabrication and optical testing.

The data for the f/12 collimator show an axial error of 4-13 mm (Figure 5). The data were fit for the position of the vertex and the radius of curvature. The conic constant and tilt of the axis are held constant. The vertex is shifted transverse to the axis by (0.072, 0.037) mm and axially by 0.012 mm. The radius of curvature is shorter by 0.18 mm.

See Table 4 for the parameters of this and the other mirrors.

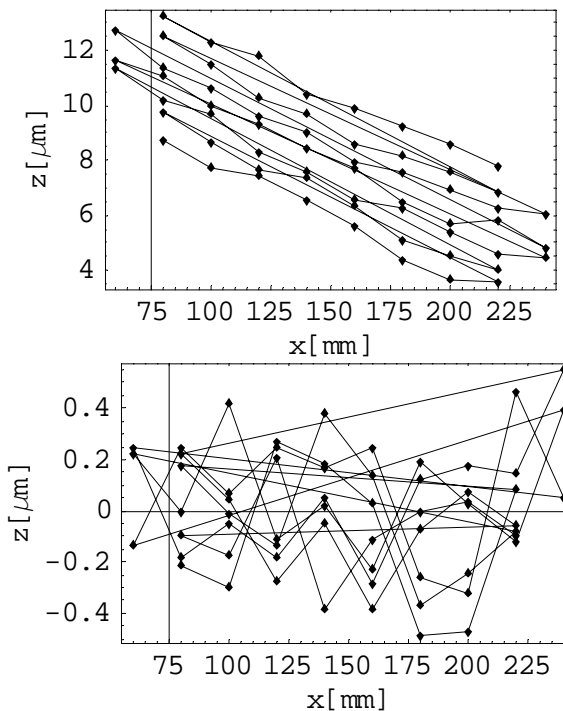


Figure 5 Top: axial distance relative to the nominal surface vs. the position from the vertex for the f/12 collimator. Bottom: fit residuals. The lines connect the points, which were taken on a raster.

Table 4 Parameters of the powered mirrors measured with a CMM. Positive x means the vertex is shifted toward the mirror center. Positive z means there is too much material. (x,y,z) is a right handed system. Positive dr means the radius of curvature is too large.

| Mirror | dx | dy | dz | dr |
|-----------|-------------------|-------------------|--------------------|-----------------|
| f/12 Coll | 0.072 ± 0.004 | 0.037 ± 0.001 | 0.012 ± 0.0002 | -0.18 ± 0.04 |
| f/12 Cam | 0.099 ± 0.005 | 0.004 ± 0.001 | -0.069 ± 0.0002 | 0.04 ± 0.05 |
| f/21 Coll | 0.063 ± 0.008 | -0.053 ± 0.001 | 0.023 ± 0.0004 | 0.04 ± 0.07 |
| f/21 Cam | -0.115 ± 0.009 | 0.147 ± 0.002 | -0.074 ± 0.0003 | -0.06 ± 0.12 |

4 Focusing

We put an artificial star at the mask, which is at the focus of the telescope and moved it to focus.

The artificial star is a $\phi 8\text{-}\mu\text{m}$ pinhole illuminated by a 632-nm laser. Because of diffraction, the beam from the pinhole illuminates the pupil, although the illumination is not uniform. The pinhole is mounted on a plate with the same curvature as the telescope image surface.

Focus is defined to be where the astigmatism is minimum. Consider a 3×3 pixel box that is centered on the image of the star. Consider the intensities $F_{i,j}$, where $i = -1, 0, \text{ and } 1$, and $j = -1, 0, \text{ and } 1$. The parameter $q_x = 1 - F_{0,0}/(F_{-1,0} + F_{0,0} + F_{1,0})$ is a measure of the sharpness in the x-direction, and $q_y = 1 - F_{0,0}/(F_{0,-1} + F_{0,0} + F_{0,1})$ is a measure of the sharpness in the y-direction.

For $f/12$, as the axial position of the pinhole changes, q_y drops and q_x rises (top panels of Figure 6). The difference $q_y - q_x$ is zero at $z = 3.03 \pm 0.06$ mm from the nominal position. The estimated standard deviation of the data is 0.02.

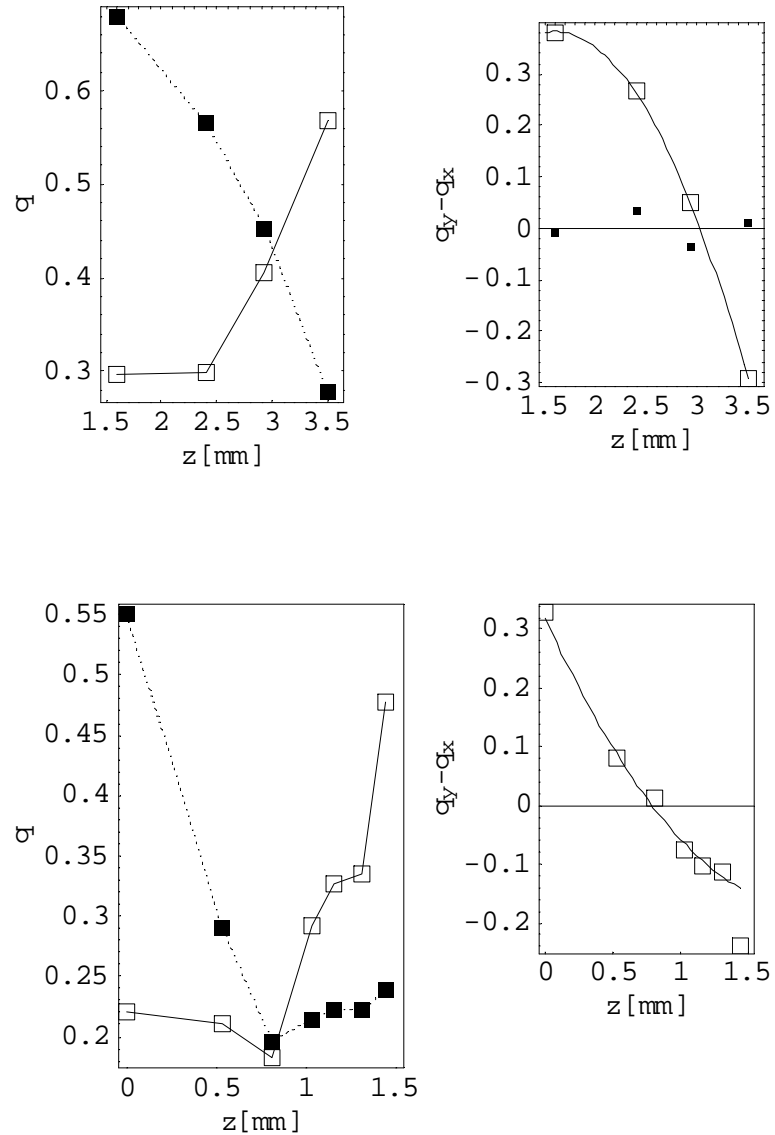


Figure 6 Image sharpness q_x and q_y vs axial position z of the pinhole (left) and difference between image sharpness $q_y - q_x$ and fit line (right). The top panels are for $f/12$; bottom panels are for $f/21$.

For f/21, the difference $q_y - q_x$ is zero at $z = 0.789 \pm 0.045$ mm from the nominal position. See bottom panels of Figure 6.

Focusing is done for a single lateral location of the pinhole. For field point $(z, x) = (-62, 17)$, which is used for f/12 focus, the location of the pinhole is at 0.3 mm (in front of the mask) relative to the position for the least astigmatism over the entire field. For field point $(-10, 10)$, which is used for f/21 focus, the location of the pinhole is 0.05 mm relative to the position for least astigmatism.

5 Accounting for Focus

Table 5 Corrections that change the focus

The focal position tests whether we have found all sources of error. To focus, the pinhole must move $dy = 3.03 \pm 0.06$ mm for the f/12 channel and $dy = 0.79 \pm 0.05$ mm for the f/21 channel. Table 5 is a list of the errors and amount of movement of the pinhole to compensate for the error.

With the errors that we have found, the residual movement of the pinhole is 0.02 mm (0.3σ) for the f/12 channel and -0.19 mm (-4σ) for the f/21 channel.

The residual for f/21 is missing the position of the f/21 collimating mirror, because its rotation stage was not available for measuring.

Because both residuals are close to zero, we believe that we have found the corrections that affect focus significantly.

| Source | Parameter | dn err | dy @ pinhole | |
|--------|-----------------------------------------------------|--------|-----------------|-----------------|
| | | | f/12 | f/21 |
| inCOB | f12Col | 0.02 | -0.02 | |
| inCOB | f12Cam | -0.12 | 0.17 | |
| inCOB | mask | 0.55 | 0.55 | 0.55 |
| inCOB | f21Cam | 0.04 | | -0.02 |
| inCOB | backFold1 wrt fold1 | 0.70 | | |
| inCOB | backFold2 wrt fold2 | 0.51 | | |
| Zemax | COB pins, alignment, mirror fab | | -0.48 | -0.31 |
| Align | 2eye tilt for f/12 image | -0.36 | 0.54 | |
| Align | 2eye tilt for f/21 image | -0.310 | | 0.168 |
| CMS | f21Cam vertex | -0.074 | | 0.040 |
| CMS | f21Col vertex | 0.023 | | -0.02 |
| CMS | f12Cam vertex | -0.069 | 0.103 | |
| CMS | f12Col vertex | 0.012 | -0.012 | |
| CMS | f12Col rad curvature | -0.18 | 0.09 | |
| Mech | image surface wrt det. carrier | -1.308 | 1.950 | 0.710 |
| Mech | det frame | 0.048 | -0.072 | -0.026 |
| Mech | lens too thick | 0.15 | 0.07 | 0.02 |
| Align | f/21Col: shift btwn use & alignment | 0.07 | | -0.07 |
| inCOB | mask tilted | | 0.03 | 0.02 |
| | f12Cam fab-design | 0.015 | -0.011 | |
| | f21Cam fab-design | -0.011 | | 0.003 |
| | pinholes (on sphere) shifted | | 0.09 | -0.07 |
| | measurement of focus | | 3.03 ± 0.06 | 0.79 ± 0.05 |
| | unaccounted | | 0.02 | -0.19 |
| dn err | Shift of optic parallel to normal | | | |
| Align | Measured during alignment | | | |
| CMS | Measurement of mirror with a CMM at CMS, Wixom, MI. | | | |
| inCOB | Measurement of location in the COB. | | | |
| Opt | Optical measurement | | | |
| Mech | Measured with coordinate-measuring machine (CMM) | | | |
| Zemax | Measured in optical design | | | |

5.1 Problems

On the collimator side, the pinhole moves $dy = -dn$ to compensate for an error dn . Being in a collimated beam, errors in the fold thickness do not affect the focus. On the camera mirror side, the pinhole moves $dy = -f^2dn$ to compensate for an error dn , where f is the ratio of the focal length of the collimator to that of the camera mirror.

5.1.1 Position Errors

The position errors (§2) will be fixed.

5.1.2 Aberrations

For the optical design, where the two major aberrations are astigmatism and field curvature, focusing means balancing the elongation of these aberrations (Figure 7). The focus moves because misplacements and tilts of the optics change the aberrations.

For the field point used for focusing the f/12 channel, the “pin hole” moves to $n = 0.48$ mm (in the direction of the normal vector of the mask) for best focus. The field point is at $(n \times z, z) = (-20.3, -51.4)$ at the mask or $(x_z, y_z) = (-5.8, -16.3)$ at the detector. For the field point used for focusing the f/21 channel, the “pin hole” moves to $n = 0.31$ mm for best focus. The field point is at $(n \times z, z) = (-11.6, -15.1)$ at the mask or $(x_z, y_z) = (-16.3, -16.8)$ at the detector.

Even without the shifts, the best focus is not the same across the field. The focus changes across the field by 100 mm for f/12 and 200 mm for f/21 (lower panels of Figure 7). This effect is measurable at wavelength 632 nm, where the test was made. Since the diffraction width is wider in the infrared, this does not degrade the image appreciably in use.

5.1.3 Cage of 2-eye Tilted

Since the cage to which the detector frames mount was tilted, the detector was shifted by an amount, which changes with the field point. The problem was that drilling the holes for the pins raised bosses around the holes. We have sanded off the bosses.

Table 6 Tilts and shifts to simulate the assembled instrument. The coordinates x and y are local Zemax coordinates.

| | dx | dy | θ_x | θ_y |
|----------|--------|--------|------------|------------|
| | mm | mm | deg | deg |
| f21 Coll | -0.053 | -0.063 | -0.026 | -0.039 |
| f12 Coll | 0.037 | 0.384 | 0.043 | 0.037 |
| fold1 | | | 0.049 | -0.007 |
| fold2 | | | 0.055 | -0.004 |
| f21 Cam | -0.147 | 0.571 | -0.021 | -0.002 |
| f12 Cam | -0.004 | 1.402 | 0.040 | -0.008 |

5.1.4 Mirror Fabrication Errors

The mirror fabrication errors (§3), which are rather small, will be subsumed in a final adjustment for focus.

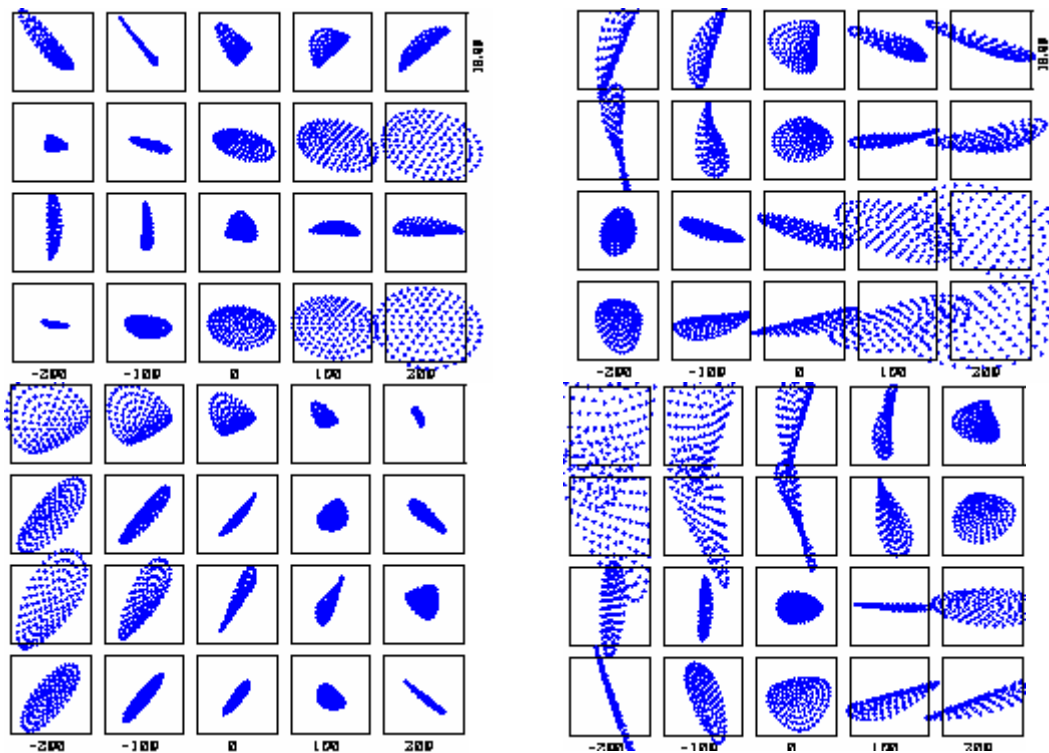


Figure 7 Through focus spot diagram for nominal $f/12$ (lower right), shifted $f/12$ (upper right), nominal $f/21$ (lower left), and shifted $f/21$ (upper left). The “pinhole” has been shifted 0.6 mm out of the instrument for the shifted $f/12$ and 0.29 mm for the shifted $f/21$. For each image, the image moves 100 mm. The box represents an 18- μm pixel. The Airy diameter (diameter of the first dark diffraction ring) at 632 nm is 0.5 pixels for $f/12$ and 0.8 pixels for $f/21$. The four fields are $(z, \text{nxz}) = (14, -14)$ mm, $(14, 14)$ mm, $(-14, -14)$ mm, and $(-14, 14)$ mm from top to bottom.

5.1.5 Offset of Detector in the Detector Package

The detector package butts against a surface of the detector frame. We had assumed that the imaging surface and the detector package are coincident. We measured that distance for the two multiplexers with a microscope with a short depth of field; we measured the distance between the visible surface

Table 7 Distance from the top surface of the detector package

| Detector | Distance [mm] to | |
|---------------|------------------|-------|
| | Surface | Image |
| Det Spec | 0.15 | 0.37 |
| Det 24 | 0.01 | 0.23 |
| Det 14 | 0.06 | 0.27 |
| Mux L1W25-B1 | 1.30 | 1.30 |
| Mux L4W451-B2 | 1.32 | 1.32 |

and the detector package for two detectors². According to the manufacturer³, there is a 0.38-mm layer of sapphire in front of the imaging surface. The optical path length is $d/n = 0.38/1.75 = 0.22$ mm below the visible surface.

5.1.6 Detector Frame

The detector mounts in a frame, the dimensions of which affect focus. The detector moves 0.048 from the nominal position in the direction of the normal to the surface. All four are essentially identical, the distance being $-0.010, 0.008, 0.008, -0.006$ mm from the average for frames 1–4, respectively.

5.1.7 Lens Thickness

We measured the thickness and other parameters of the field-flattening lenses. The thickness causes a shift in focus, which is detectable in focusing.

Table 8 Measured parameters in mm of the field-flattening lenses, expresses as the deviation from the nominal values

| Lens | Thickness | RadCurv | Diam | Centering | dFocus |
|------|-----------|---------|--------|-----------|--------|
| Nom | 5.300 | 150.000 | 65.000 | 0.000 | |
| 1 | 0.140 | -0.129 | -0.111 | 0.058 | 0.047 |
| 2 | 0.160 | -0.207 | -0.095 | 0.046 | 0.053 |
| 3 | 0.126 | -0.016 | -0.040 | 0.073 | 0.042 |
| 4 | -0.077 | -0.476 | -0.078 | 0.029 | -0.026 |

5.1.8 Pinholes Shifted

To mimic the curved image surface of the telescope, the pinholes are mounted in recesses on a plate (Figure 8). Because multiplexer L1W25-B1 is offset in the package, the plate was shifted from the nominal location to make the image fall on the detector. This caused a shift in focus.

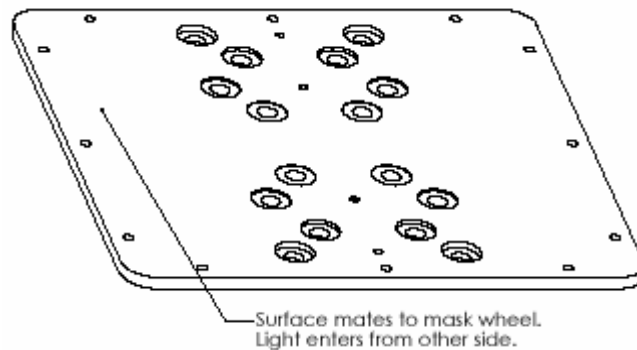


Figure 8 Mask plate showing recesses, which create a curved surface for pinholes

² Davis, M, & Loh, E., 2001, "Detector Metrology, Spartan IR Camera for the SOAR Telescope," www.pa.msu.edu/~loh/SpartanIRCamera/detectorMetrology.pdf

³ Haas, Allen, 2002 "Users Guide for the HAWAII-2 2048x2048 Pixel Focal Plane Array," Rockwell Scientific Company, LLC.

5.1.9 Other Problems Caused by Looseness in the Rotation Stages

The looseness of the rotation stages caused the shift between alignment and use of the f/12 camera and f/21 collimator, the tilted mask, and part of the errors in the positions of the optics measured in the COB. With the remanufactured, tight rotation stages, these problems will be gone.